Engineering Science and Technology, an International Journal 24 (2021) 694–705

HOSTED BY

Contents lists available at ScienceDirect

Engineering Science and Technology, an International Journal

journal homepage: www.elsevier.com/locate/jestch

Full Length Article

Improved finite control set model predictive control for distributed energy resource in islanded microgrid with fault-tolerance capability

Hussain Sarwar Khan [a,*], Muhammad Aamir [b], Kimmo Kauhaniemi [c], Mohsin Mumtaz [d], Muhammad Waqar Hassan [d], Muhammad Ali [d]

[a] School of Technology and Innovation, University of Vaasa, Finland
[b] Pak-Austria Fachhochschule, Institute of Applied Sciences and Technology, Haripur, Pakistan
[c] School of Technology and Innovation, University of Vaasa, Finland
[d] Department of Electrical Engineering, Bahria University, Islamabad, Pakistan

ARTICLE INFO

Article history:
Received 12 July 2020
Revised 1 November 2020
Accepted 13 December 2020
Available online 20 February 2021

Keywords:
Distributed energy resource
Fault-tolerance capability
MPC
Microgrid

ABSTRACT

In this paper, improved finite control set model predictive voltage control (FCS-MPVC) is proposed for the distributed energy resource (DER) in AC islanded microgrid (MG). Typically, AC MGs have two or more power electronic-based DERs, which have the ability to maintain a constant voltage at the point of common coupling (PCC) as well as perform power sharing among the DERs. Though linear controllers can achieve above-mentioned tasks, they have several restrictions such as slow transient response, poor disturbance rejection capability etc. The proposed control approach uses mathematical model of power converter to anticipate the voltage response for possible switching states in every sampling period. The proposed dual-objective cost function is designed to regulate the output voltage as well as load current under fault condition. Two-step horizon prediction technique reduces the switching frequency and computational burden of the designed algorithm. Performance of the proposed control technique is demonstrated through MATLAB/Simulink simulations for single distributed generator (DG) and AC MG under linear and non-linear loading conditions. The investigated work presents an excellent steady state performance, low computational overhead, better transient performance and robustness against parametric variations in contrast to classical controllers. Total harmonic distortion (THD) for linear and non-linear load is 0.89% and 1.4% respectively as illustrated in simulation results. Additionally, the three-phase symmetrical fault current has been successfully limited to the acceptable range.

1. Introduction

Microgrid (MG) is one of the fundamental technologies, which makes the electrical power systems more intelligent, flexible and distributed. The incursion of distributed energy resources (DERs) is possible in conventional power system. Basically, MG is a localized cluster of adaptive loads, energy storage systems, and distributed generations (DG) with their effective control operating in the coordinated pattern. It can operate in islanded and grid-connected (GC) mode or both. In GC mode, MG provides auxiliary services to power systems such as voltage support, peak load shaving and load shifting [1–3]. In the case of isolation from the utility grid due to fault, regular maintenance or low power quality, MG provides high-quality power to the load in standalone mode [4]. The standalone mode can be further classified into two categories in the context of time. Temporary standalone mode occurs due to pre-planned maintenance or due to spontaneous failure in transmission lines between MG and utility grid while the permanent islanded mode is created to feed the remote communities, where power from the electrical grid is unfavorable and uneconomical [5]. In this study, permanent islanded MG is considered.

Direct current (DC) MG has more appealing features in terms of efficiency and control simplicity than AC MG however, majority of loads requires AC supply [6,7]. Consequently, it is mandatory to establish AC MG architecture which can provide regulated power with effective control. AC and DC parts of MG are interfaced through voltage source converters (VSC) [8,9]. For critical load applications, parallel operated VSCs provide high redundancy, high reliability, and more flexibility. In many cases, it is viable to distribute high power load between several VSCs instead of using a

* Corresponding author.
E-mail addresses: hussain.khan@uwasa.fi, hussainsarwar1994@yaho.com (H.S. Khan), muhammad.aamir@fecid.paf-iast.edu.pk (M. Aamir), Kimmo.Kauhaniemi@uwasa.fi (K. Kauhaniemi), mohsin143.comsats@gmail.com (M. Mumtaz), mwaqarhassan53@gmail.com (M.W. Hassan), m.turi21@gmail.com (M. Ali).

https://doi.org/10.1016/j.jestch.2020.12.015
2215-0986/

single power device with high rating. Commonly, VSCs connected in parallel and feeding a common load form an AC MG.

For the parallel operation of multiple DGs in islanded mode, many control schemes have been proposed in the literature like, average load-sharing technique [10], master–slave control [11,12], centralized based-control [13,14], etc. Though above-mentioned control techniques involved a communication structure among the DGs for smooth operation, using these techniques increase the system's complexity and reduces the reliability. Consequently, it is necessary to use a technique like droop control to govern the power-sharing between the DGs. In [15], the authors present the analysis of the droop control. It is advantageous to design a decentralized controller i.e. no external communication network between VSC-based DGs. The objectives of droop control in AC MG are power sharing among the DGs in AC MG and regulating the frequency and voltage at the AC bus.Droop control serves as an outer loop of VSC while the voltage control technique is used in the inner control loop of VSC in MG.

Various linear controls with pulse width modulation (PWM) are widely found in literature like PI, PR, PID [16,17], but, the linear control techniques have many practical restrictions such as their inability to track the sinusoidal reference with zero steady-state error, tuning of gains, poor disturbance rejection capability and incapability to handle the non-linearities of the power system [18]. Therefore, non-linear control techniques such as $H\infty$ [13], deadbeat [19,20],μ-synthesis [12], and slide mode control (SMC) [21,22] are vastly used by the power electronics industry. In[19], deadbeat (DB) control has been proposed, which moves all the system poles at zero axis line. consequently, the error drops to zero in no time thus, providing fastest dynamic response towards achieving stability. Still, its key shortcomings are parametric variations, external disturbances, and measurement noise. Observer-based DB control is proposed in [20] to increase the system stability but there is a trade off between system stability and performance of control parameters.

Another approach is $H\infty$ which effectively handles the system uncertainties,it working principle based on the hysteresis. Using the feedback loop, control action ensure position the state variable with in the hysteresis but it's variable switching frequency causes a severe stress on switches and reduces the inverter's life, thus making the filter design a bit complicated [23].μ-synthesis guarantees only local stability [24].

In comparison to linear controllers, Non-linear controllers such as slide mode control (SMC) is based on variable structure control theory. Its basic principle is divided into 2 stages. In start, the system states trajectory is forcefully taken into user-defined sliding layer, this phase is known as reaching phase then state trajectories remains in the layer and known as sliding phase. It has better performance, is robust against parametric variations, and possesses magnificent transient response under different loading conditions. Still, chattering phenomena, high switching losses and its complex mathematical modeling are the main barriers in its implementation[25,26]. Artificial intelligence-based approaches i.e. using neural networks [27], fuzzy logic and interactive learning control [28] have the ability to enhance the controller's steady-state performance. However, the approaches illustrate slower transient response and needs much time in training of models. So, an amalgam of the different control approaches balancing out their disadvantages is also found in literature [29].

FCS-MPC is a digital control method and its basic principle is different from linear control. It uses the discrete time model of VSI along with its filter to anticipate the behavior for all possible input combinations. One of the inputs having the least value of the predefined cost function (CF) is selected and applied to the coming sampling instant despite drafting a separate loop for each controlled variable and cascading them together. CF is basically, a square of the Euclidean distance between controlled and reference signal. Current observer-based MPC is proposed in [30]. The authors claim that the cost of system decreases but its performance is poor in term of THD under normal load conditions. Current sensor-less MPVC is proposed for inverter instead of measuring the inductor current. It is assumed that the system cost and computational burden have been reduced, but the proposed control scheme has not shown an effective performance under transients and the authors have not investigated the performance of the system under fault conditions [31]. In [32], predictive control is proposed using improved stationary reference frame, but the performance of control technique for the non-linear load is not investigated. In [33], an implicit VMPC is proposed for power converter with LC filter in autonomous mode, but this approach shows vulnerability to parametric variations and external uncertainties. Likewise, it requires high computational time as compared to other MPC-based approaches. In [34], VMPC for parallel connected UPS is proposed to increase the stability of the system and to reduce the system cost. Due to its robustness, outstanding transient behavior and easy addition of restraints makes FCS-MPC becomes the best alternative for the control of power converters and it can be implemented to a vast range of power electronic applications [35].

The power system faults are further divided into two categories i.e. Symmetrical and unsymmetrical faults. All three phase to ground short circuit is known as symmetrical fault while single phase to ground or two phase to ground short circuits are lies in unsymmetrical faults type. However symmetrical faults are more sever than unsymmetrical faults. This study focuses on the symmetrical faults. Ideally under fault and overload conditions, VSI Output current remains in limit to restrain the damage of the VSI's switches because the converter has low thermal inertia.Normally, the output current increases up to three times of the load current.In order to reduce the damage usually latched limit and instantaneous saturation limit techniques is used. In latched limit, a predefined current reference is introduced in place of actual reference and voltage loop is disconnected due to change of reference. Converter voltage becomes distorted and increases in healthy phases. while in instantaneous saturation strategy, a limiter is added to limit the current. however, this method is easy to implement but output becomes distorted for sinusoidal signal. In [36] a virtual resistance is introduced to reduced the reference current but this technique also reduces the system output voltage.In [37] current limit control based on Instantaneous saturation is proposed for parallel UPS, working in master–slave configuration. The reference for slave converter is generated by master converter by reducing the reference amplitude. consequently the quality of current wave becomes distorted.It also required the communication setup.To limit the fault current, harmonics components of power is used to generate the current reference for grid-tied inverter and proposed in [38].In [39] hardware components is used to limit the current under faults conditions. Hardware based along with instantaneous limit technique is proposed in [40]. although implementation of external devices increases the system cost and reduce the reliability and reduction of the fault limiter size is an important factor to be considered.

Table 1 shows the summary of above discussed control techniques based on parameter, which is used to analysis the performance of control techniques. The linear control scheme is mature and well recognized in literature and extensively uses by PE industry. Instead of that, modern control techniques include new ideas, complex mathematical modeling, the frame of reference transformation, and the often-required microprocessor. Among control schemes, hysteresis control has the easiest approach. System data is not required for the hysteresis and ANN control. But ANN control demands the preceding information and perception of designers

Table 1
Overview of advanced control techniques.

	Linear control	Dead-beat	Slide mode control	ANN	Model predictive control
	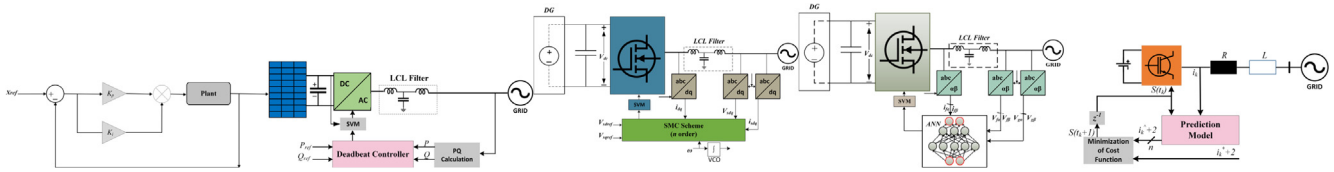				
Theoretical background	Strong	Moderate	Strong	Weak	Strong
Stability analysis tools	Strong	Strong	Strong	No	Initial Results
Computational complexity	Low	Average	Medium	Low	High
Intuitive design	Low	Average	Medium	Low	High
Handling system constraints	No	No	No	Yes	Yes
Handling non-linearities	No	Yes	Yes	Yes	Yes
Parameter sensitivity	Strong	Average	Robust	Data Dependent	Tunable
Fault tolerance capability	No	No	Yes	Not-studied	Yes

and its performance is directly related to training data. The constraints are handle by the ANN and MPC.ANN is newly introduced in the power electronics domain and have weak theoretical literature. The response of hysteresis and MPC has exceptional performance under different loading conditions. SMC required complex mathematical modeling and has high computational burden. Despite high computational burden. MPC is better in all aspects discussed in 1.

This paper presents an improved voltage control strategy for VSC in order to regulate the output voltage of single and parallel DG units operating in an islanded mode of MG. The key contributions in this paper includes;

1. A dual objective cost function-based two-step prediction horizon FCS-MPVC for single DG in the islanded mode.
2. The systems mathematical model is used to predict the imminent action of the system for possible switching sequences in a sampling period.
3. The cost function is designed to determine the optimum action and then it is applied to the coming sampling period.
4. A two-step prediction horizon-based CF is formulated to decrease the converter switching frequency and also to increase the system efficiency.
5. In order to control fault current under fault condition, a dual-objective cost function is designed, the primary objective of the CF is to compensate the voltage error and its secondary function is to control the current under fault conditions.

Proposed control technique is validated for single DG under linear, non-linear, and unbalance loading condition. More importantly, the controller exhibits efficient performance under fault condition. Similarly, multiple DGs parallel operation has been simulated for the proposed control and droop technique is analyzed for accurate power sharing.

The remaining paper is arranged as follows. The proposed control strategy is explained while providing the comprehensive mathematical model of two-level VSC with linked LC filter and discussing the discretization aspects of FCS-MPC implementation in Section 2. Further, the FCS-MPC operating principle is explained in this section. Cost function design is explained in Section 3 while Section 4 presents the switching reduction mechanism. The Section 5 explains the droop control for proper power sharing between the DGs and its restrictions are also presented. In Section 6, the detailed simulation results are explained. Finally, the last section comprises of the conclusion.

2. Mathematical modelling of DER system

A detailed block diagram of MG having renewable energy resources connected with AC bus through PE interface, each converter have it's own primary and secondary control and also connected with MG central controller for the smooth operation of MG is illustrated in 1. The MPC uses the discrete time converter model and its filter parameters to find the optimal action by minimizing the CF. Based on minimized CF, optimal control action is anticipated for the next sampling time. Precise mathematical model of the VSC and filter is required to attain good control performance. Particularly in AC MG, two-level VSC topology is used as shown in 2. The output LC filter is used to eliminate the high frequency current components which are undesirable. VSC modelling is done in the stationary orthogonal frame of reference. The two assumptions are considered i.e. the VSC is in balanced condition and all three phases are balanced.Three phases x-y-z are transformed into $\alpha\beta$ frame by using the Clarke transformation: see Fig. 3.

(2)

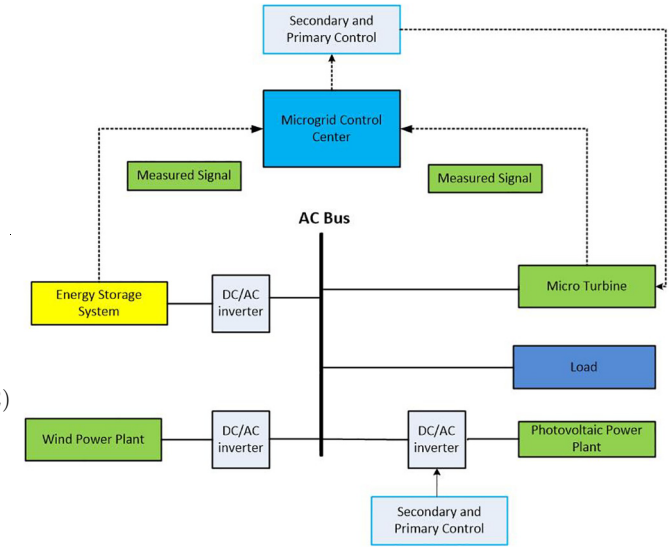

Fig. 1. Islanded MG contains three DG's with VSI and different type of loads.

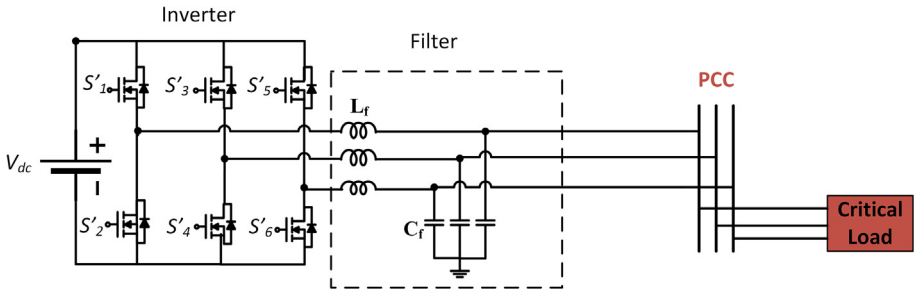

Fig. 2. Circuit representation of 3-phase VSC with output LC filter connected with load at PCC.

$$T = \frac{1}{3}\left[e^{j}\frac{2}{3}\pi e^{j}\frac{2}{3}\Pi\right] \tag{3}$$

2.1. Converter model

The converter consists of three legs $(S_x, S_y, S_z)$and each leg has two switches so there are two possible switching states for each leg, which are described below:

$$S_x = \left\{\begin{array}{ll} 1, & S'_1 \text{ is ON and } S'_4 \text{ is OFF} \\ 0, & S'_1 \text{ is OFF and } S'_4 \text{ is ON} \end{array}\right\} \tag{4}$$

$$S_y = \left\{\begin{array}{ll} 1, & S'_2 \text{ is ON and } S'_5 \text{ is OFF} \\ 0, & S'_2 \text{ is OFF and } S'_5 \text{ is ON} \end{array}\right\} \tag{5}$$

$$S_z = \left\{\begin{array}{ll} 1, & S'_4 \text{ is ON and } S'_6 \text{ is OFF} \\ 0, & S'_4 \text{ is OFF and } S'_6 \text{ is ON} \end{array}\right\} \tag{6}$$

However, two-level VSC has eight possible switching arrangements. The voltage between N-th point and leg can be computed

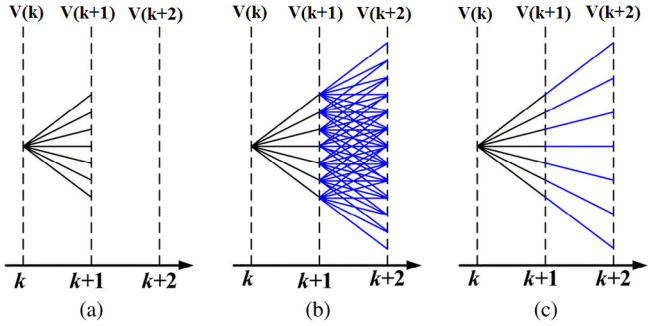

Fig. 3. Demonstration of prediction approach. (a) N = 1, (b) N = 2, In every sampling time, different voltage vectors are using. (c) N = 2, but same vector is taking into account for two consecutive sampling time.

by taking the product of the DC link voltage with the present state of the corresponding leg:

$$\begin{aligned} V_{xN} &= S_x.V_{dc} \\ V_{yN} &= S_y.V_{dc} \\ V_{zN} &= S_z.V_{dc} \end{aligned} \tag{7}$$

The voltage between phase to neutral (from x, y, z to n-th point) is determined by subtracting the common voltage from 7. Common voltage is determined by executing Kirchhoff's voltage law:

$$V_{nN} = \frac{V_{xN} + V_{yN} + V_{zN}}{3} \tag{8}$$

Phase voltage is:

$$\begin{aligned} V_{xn} &= V_{xN} - V_{nN} \\ V_{yn} &= V_{yN} - V_{nN} \\ V_{zn} &= V_{zN} - V_{nN} \end{aligned} \tag{9}$$

Clark transformation is applied to find eight possible switching states. These are expressed in Table 2.

2.2. Filter modelling

To suppress the switching harmonics, a LC filter is coupled at VSC's output terminal as illustrated in 2. LC filter has an inductor L_f, and capacitor C_f and damping resistance R_f with current I_f and voltage V_{pc} across the load. I_f and $_{V_{pc}}$ are the state variables in this system. The Eq. 10 and 11 explain the filter dynamics. Inductive behaviour of the filter is described in 10, while 11 demonstrates the capacitive response of the filter. The equations are stated as:

$$L_f \frac{d_{i_f}}{d_t} = v_t - v_{p_c - i_f R_f} \tag{10}$$

$$C_f \frac{d_{V_{pc}}}{d_t} = i_f - i_0 \tag{11}$$

$$\frac{d}{d}\begin{bmatrix} i_f \\ V_{pc} \end{bmatrix} = \mathbf{A}\frac{d}{d}\begin{bmatrix} i_f \\ V_{pc} \end{bmatrix} + \mathbf{B}\frac{d}{d}\begin{bmatrix} v_t \\ i_0 \end{bmatrix} \tag{12}$$

$$\mathbf{A} = \begin{bmatrix} \frac{-R_f}{L_f} & \frac{-1}{C_f} \\ \frac{1}{C_f} & 0 \end{bmatrix} \tag{13}$$

Table 2
Feasible switching sequence for power converter.

Space-Vector		On-state switches	Vector placing
Zero vector	$\vec{V_{0,7}}$	S'_1, S'_3, S'_5	$\bar{v_{0,7}} = 0$
Active Vector	$\vec{V_1}$	S'_1, S'_6, S'_2	$\bar{v_1} = \frac{2}{3} v_{dc}$
	$\vec{V_2}$	S'_1, S'_3, S'_2	$\bar{v_2} = \frac{1}{3} v_{dc} + j\frac{\sqrt{3}}{3} v_{dc}$
	$\vec{V_3}$	S'_4, S'_3, S'_2	$\bar{v_3} = -\frac{1}{3} v_{dc} + j\frac{\sqrt{3}}{3} v_{dc}$
	$\vec{V_4}$	$S'_{44}, S'_{33}, S'_{55}$	$\bar{v_4} = -\frac{2}{3} v_{dc}$
	$\vec{V_5}$	S'_4, S'_3, S'_5	$\bar{v_5} = -\frac{1}{3} v_{dc} - j\frac{\sqrt{3}}{3} v_{dc}$
	$\vec{V_6}$	S'_1, S'_4, S'_5	$\vec{v_6} = \frac{1}{3} v_{dc} - j\frac{\sqrt{3}}{3} v_{dc}$

$$\mathbf{B} = \begin{bmatrix} \frac{1}{Lf} 0 \\ 0 \frac{-1}{Cf} \end{bmatrix} \tag{14}$$

2.3. Discrete time modelling of the LC filter

For the practical implementation of the proposed control approach on digital control platforms, continuous time state space (CTSS) model of the filter is essentially converted into discrete time state space (DTSS) model. In order to convert the model to DTSS, different discretization techniques are used, but in this study, Zero order-hold technique is implemented. Actually, Zero order-hold technique is implemented. Actually, it provides the exact transformation of CTSS to DTSS model for each sampling period in stair type inputs. In this paper, the value of the dc-link voltage V_{dc} is taken constant and the mathematical model of the DTSS is described as:

$$\begin{bmatrix} i_f(t_{k+1}) \\ V_{pc}(t_{k+1}) \end{bmatrix} = A_d \begin{bmatrix} i_f(t_{k+1}) \\ V_{pc}(t_{k+1}) \end{bmatrix} + B_d \begin{bmatrix} v_t(t_k) \\ i_0(t_k) \end{bmatrix} \tag{15}$$

$$A_d = e^{AT_s} \tag{16}$$

$$\mathbf{B}_d = \int_0^{\vec{T_s}} e^{A\tau} B d_\tau \tag{17}$$

T_s is the sampling instant. It is assumed that T_s is very small so the exponential matrix is approximated as:

$$e^{AT_s} = 1 + AT_s \tag{18}$$

By using 15, the capacitor voltage at instant (t_{k+1}) is determined by the following equation:

$$v_{pc}(t_{k+1}) = v_{pc}(t_k) + \frac{T_s}{C_f}\left(i_f(t_k) - i_0(t_k)\right) \tag{19}$$

19 is used to find the voltage at the next sampling instant.

3. Cost function

The working of investigating MPVC algorithm is briefly explained below:

- $v_{pc}, i_f$and $i_0$are measured through sensors in the beginning of every sampling period.
- The measured values of voltages and currents are used to anticipate system variable via (19), for all probable switching arrangements.
- Pre-defined CF (21) or (22) is evaluated using predicted state values (19) then switching pattern (Table 1) at which CF has minimal value. It is applied to converter in coming sampling instant.

In order to implement FCS-MPC, CF formulation is fundamental. Basically, CF gives the error between the reference and the forecast value. MPC can handle the multiple objective based-issues.By defining these in cost function as expressed in 20:

$$g_{Gen} = \sum_{i=t_k}^{t_k+N-1} \left\| v_{fe}(i) \right\|_2^2 + h_{lim}(i) + \lambda_u sw^2(i) \tag{20}$$

$v_{fe}(i)$ is the anticipated tracking error,$h_{lim}(i)$ is the current limitation, $sw^2(i)$defines the reduction of switching frequency and is regulated by weighting factor λ. CF employed in the study is expressed in 21. It is a specialized type of 20 with $N = 2$, Its primary role is to lessen the Euclidean distance at every sampling instant. CF used in this study is described below:

$$g_v = \left(v^*_{(pc)}\alpha(t_{k+2}) - v_{(pc)\alpha}(t_{k+2})\right)^2 + \left(v^*_{(pc)}\beta(t_{k+2}) - v_{(pc)_\beta}(t_{k+2})\right)^2 \tag{21}$$

$v^*_{(pc)}\alpha$and $v^*_{(pc)}\beta$ are real & imaginary parts of the voltage reference at t_{k+2} instant, usually provided by the droop approach in AC MG.$v_{(pc)_\alpha}$ and $v_{(pc)_\beta}$ are anticipated output voltages at the t_{k+2} instant. Above defined CF provides us a voltage error.

3.1. Dual-objective cost function for symmetrical fault

Basically, dual objective cost function is designed to regulate the AC bus voltage and also to minimize the fault current under fault conditions. The dual objective cost function is defined as:

$$G_{DO} = \left(v^*_{(pc)_{\alpha\beta}}(t_{k+2}) - v_{(pc)_{\alpha\beta}}(t_{k+2})\right)^2 + \left(i^*_{(f)_{\alpha\beta}}(t_{k+1}) - i_{(f)_{\alpha\beta}}(t_{k+1})\right)^2 \tag{22}$$

Load current term is introduced in the new CF to regulate the load current under fault conditions. By introducing the new term of the current in CF as mentioned in 22, There is a trade-off between voltage quality in terms of THD and the current waveform, but the THD of voltage slightly increases whereas the current waveform remains sinusoidal and surge in a current is limited under fault conditions. Consequently, the advantages of addition of a new term outweighs its disadvantages. Among all the voltage vectors, the vector which has minimum value of g_v is applied to the next sampling instant.

4. Switching frequency reduction scheme

The switching frequency of the converter plays a vital role in power generation. If the switching frequency is high, more losses will occur. Consequently, efficiency of the system decreases and vice versa. In this study, a two-step prediction horizon approach is realized to attain low switching frequency for better efficiency. If one-step prediction horizon is taken into account, only eight possible voltage vectors are estimated for each sampling instant. For the implementation of the prediction horizon where N = 2, two voltage vectors are evaluated. One voltage vector is determined for the 1st sampling period and other vector is applied for the 2nd sampling period. So, 49 combinations of voltage vectors are possible and may be determined as demonstrated in Fig. 3b. This scheme increases the computational burden, which causes problems in implementation stages.

To lessen the switching frequency, a simple two-step prediction is implemented in this paper. For both sampling periods, the same voltage vector is determined [41]. Subsequently, only 7 voltage vectors are evaluated instead of 49 vectors for both sampling instants, as illustrated in Fig. 3c. The implemented scheme gives same performance with very low switching frequency. Voltage for instant t_{k+2} is anticipated by using 19. This approach lowers the switching frequency and also reduces the voltage ripples and increases the wave quality.

5. Droop control

Originally each DG is designed to generate a power according to its reference at base frequency i.e. 60 Hz in this study. In the case of islanded MG, the main aim of the local controller of DG is to com-

pensate the voltage and frequency within MG. But there is a need of secondary controller to control the voltage and frequency of MG. Droop control is extensively adopted in MG to control the voltage and frequency, as well as proper sharing of active and reactive power between the DGs [24]. In this work, droop control is used for accurate sharing of the active and reactive power of each DG proportional to its ratings. Droop control can be expressed as follows:

$$V_{ref} = V_{nom} - k_q Q_{cal} \tag{23}$$

$$f_{ref} = f_{nom} - k_p P_{cal} \tag{24}$$

where as $f_{ref}$and V_{ref} are reference frequency and voltage respectively used to determine the $V_{ref,\alpha\beta}$. $V_{nom}$and f_{nom} are nominal voltage and frequency respectively. Following equations are used to calculate the active power P_{cal} and reactive power Q_{cal}.

$$P_{cal} = v_{pc,\alpha} i_{0,\alpha} + v_{pc,\beta} i_{0,\beta} \tag{25}$$

$$Q_{cal} = v_{pc,\beta} i_{0,\alpha} - v_{pc,\alpha} i_{0,\beta} \tag{26}$$

Low-pass filter is used to mitigate the harmonics in the calculated power. However, it shows slow-response under step change of load. k_q and k_p are droop power coefficients. Basically, voltage control and coefficients of droop are inversely proportional. Hence, adjustment between both the parameters is essential to find an optimal solution. The slope of the droop curves are also calculated using droop coefficients and expressed as:

$$k_q = \frac{\delta V}{Q_{max}} \tag{27}$$

$$k_p = \frac{\delta f}{P_{max}} \tag{28}$$

ΔV and Δf represent the allowable variations in voltage and frequency respectively. Q_{max} and P_{max} are the nominal active and reactive power provided by the system.Control technique expressed in (23) and (24) is commonly known as droop control as expressed in Fig. 4. Table 3 presents the comparison among the resistive-impedance and inductive-impedance based droop approach. see Fig. 5–7

Table 3
Evaluation among different impedance-based droop control.

Parameter	Resistive type $\varnothing = 90^{\circ}$ Z = r	Inductive type $\varnothing = 90^{\circ}$ Z = jx
Active power	$P = \frac{EV\cos\varnothing - V^2}{r} \cong \frac{v}{r}(E - v)$	$P = \frac{EV}{X}\sin\varnothing \cong \frac{EV}{X}\varnothing$
Reactive power	$Q = -\frac{ev}{R}\sin\varnothing \cong \frac{ev}{r}\varnothing$	$Q = \frac{ev\cos\varnothing - v^2}{x} \cong \frac{v}{x}(e - v)$
Frequency Equation	$\omega - k_P Q = \omega^*$	$\omega + k_P P = \omega^*$
Amplitude equation	$E = E^* - k_Q P$	$E = E^* - k_Q Q$
Droop coefficient	$k_P = \frac{\Delta\omega}{Q_N}$	$k_P = \frac{\Delta\omega}{P_N}$
Droop coefficient	$k_Q = \frac{\Delta E}{P_N}$	$k_Q = \frac{\Delta E}{2Q_N}$

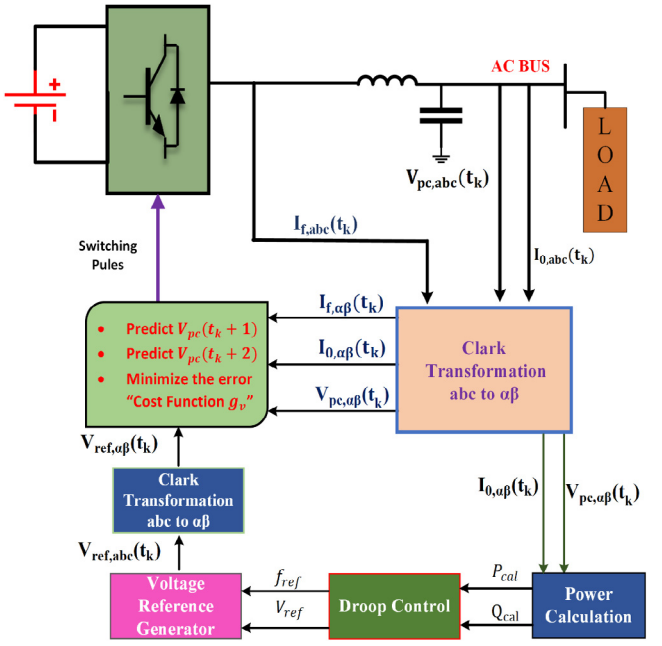

Fig. 5. Block diagram of investigating control scheme along with droop control in islanded mode of MG.

6. Simulation: results & discussion

For the validation of the proposed control technique, extensive real-time simulations are carried out in MATLAB/Simulink for both single DG and parallel DG in islanded MG. Different simulation scenarios are simulated under different loading & fault conditions to present the robustness and effectiveness of the control strategy under study. Both linear and non-linear as well as unbalanced loads are considered in this study. Linear load consists of three phase RL load with the active and reactive power of P = 18 kW and Q = 7 kVar respectively. Fig. 5 presents the complete block diagram of VSC along with its control structure. First, steady-state simulation for an VSI has been done to authenticate the performance of the proposed controller under sinusoidal voltage reference. Then, transient conditions, a step change of load, and system performance under non-linear load is inspected to illustrate the system robustness and stability. Finally, two DERs with proposed controller are connected in parallel to serve the common load at AC bus in islanded MG. Accurate power sharing between the DGs are achieved by applying the droop approach. Different parameters used in this study is given in Table 4.

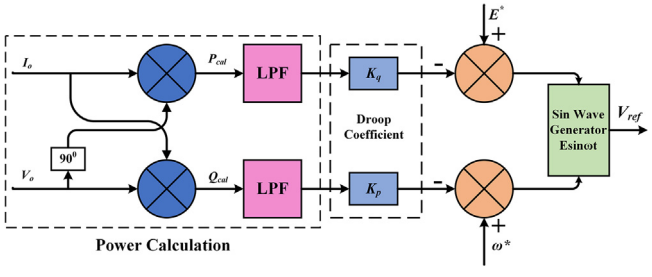

Fig. 4. Droop control.

6.1. Steady state analysis

Fig. 6 presents the results of a DG under linear RL balanced load, when RL load is connected. During operation, 18 kW active and 7 kVar reactive power is generated by the DG to meet the load demand. Both voltage and current are sine waves with negligible distortions. The execution of the proposed control scheme is equated with the standard literature [33]. In [33], output voltage THD is 2.93%. However, the proposed strategy reduces the output voltage THD to 0.89% and also with in the limit of IEEE criterion. Fig. 7 illustrates the simulation results of the voltage and current waveform for single

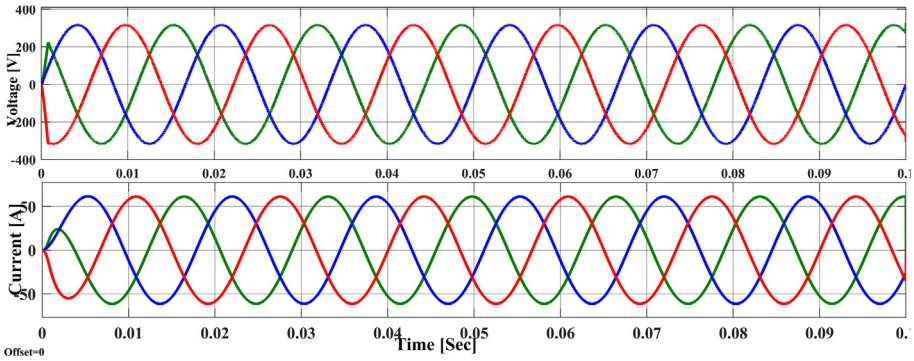

Fig. 6. Load current and output voltage of single DG under linear load.

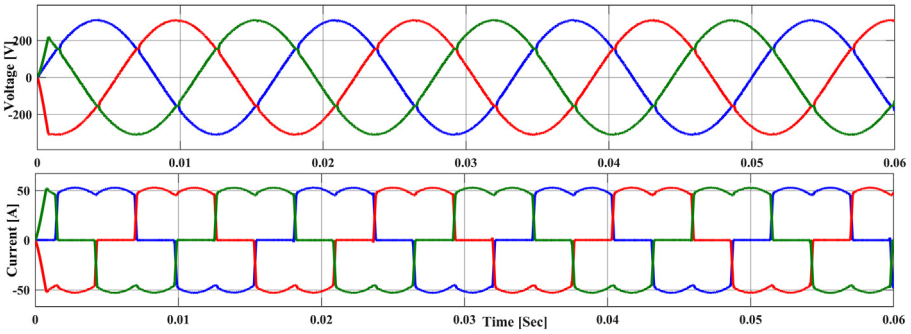

Fig. 7. Load current and output voltage of single DG under non-linear load.

Table 4
Simulation parameters.

Parameters	Values
DC link voltage	$v_{dc} = 1000$ V
Sampling time	$T_s = 20$ μ S
LC-filter	$C_f = 250$ μ$F, L_f = 2$ mH
Damping resistance	$R_f = 0.94$ W
Linear loads	$P = 18$ kW, $Q = 7$ kVar
Non-linear load (diode rectifier)	$P = 10$ kW, $Q = 4$ kVar
Nominal voltage	$V_{nom} = 311$ V
Rated frequency	$F_{ref} = 60$ Hz
Droop coefficients	$k_q = 0.008$ $k_p = 0.001$
PI parameter	$K_P = 42$ $K_I = 0.15$

DG under non-linear load condition with proposed controller. It should be seen in results that the voltage wave is a sine wave even now with THD of 1.40% regardless of the distorted output current.

6.2. Load transients studies

The load transient analysis of the system with proposed controller is performed to determine the system transient response and overshoot under varying load conditions. Fig. 8 illustrates the transient response of the system under step change in load from 0% to 100% and 100% to 0%. At time 0.1s system load becomes zero or under no load condition and a smaller spike of voltage is shown in the magnified window.which occurs due to switching of the load. However, this spike cannot create produce the stress on the switches of VSI. Then at time is 0.15s, load is again con-

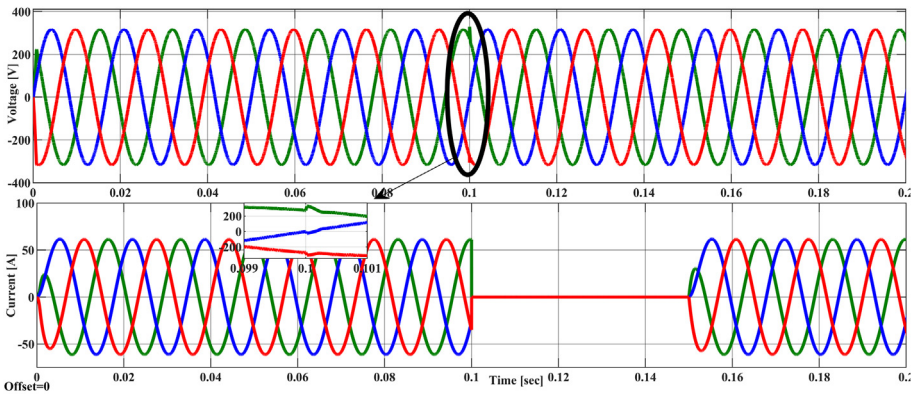

Fig. 8. Output voltage and line current results for load variations.

nected with the system. During the whole period, the output voltage of the system remains stable and the output current varies with the load. Fig. 9 demonstrates the simulation results with PI controller as a voltage regulator. At time 0.5s, extra load is added to in the system to observe the behavior of PI. Due the increase in load, a voltage dip is observe along with the distortion in current wave. The controller takes time regain its position and to start work smoothly. The THD of voltage, in the case of PI is above 4%. To validate the performance of the proposed controller, step change in load test under non-linear loading condition is per-

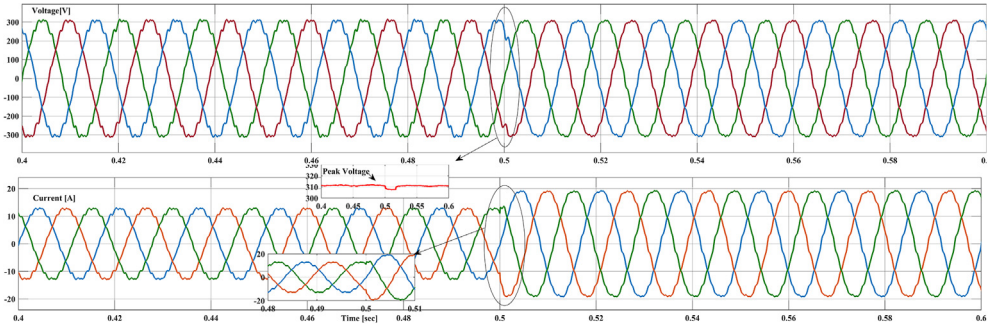

Fig. 9. Output voltage and line current results for load variations, when PI controller is employed.

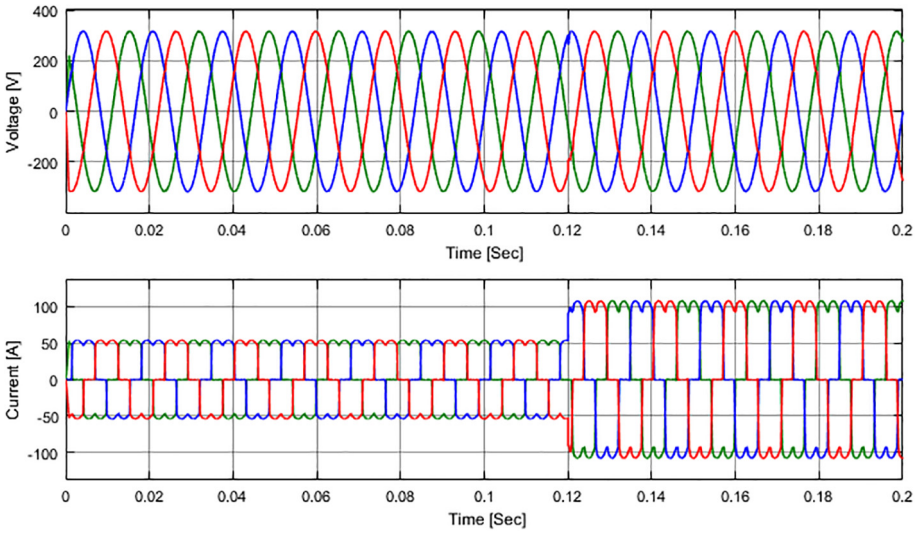

Fig. 10. Voltage and current results in step change of load.

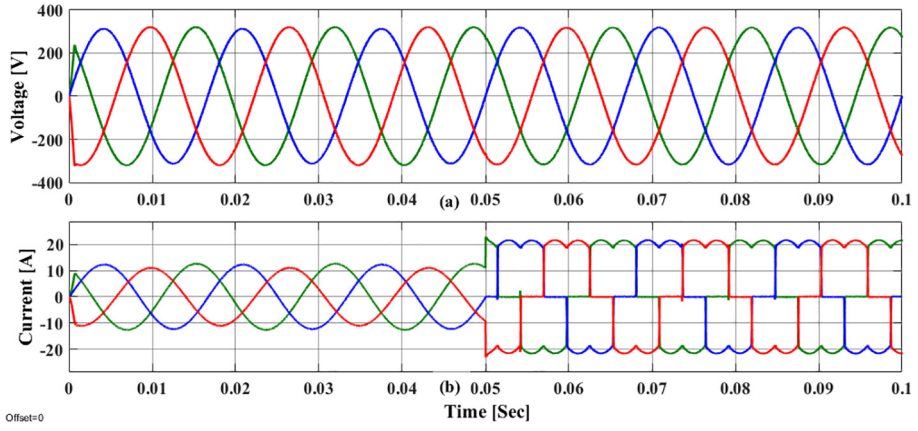

Fig. 11. Simulation results of voltage and current under unbalanced and non-linear loads using MPC controller.

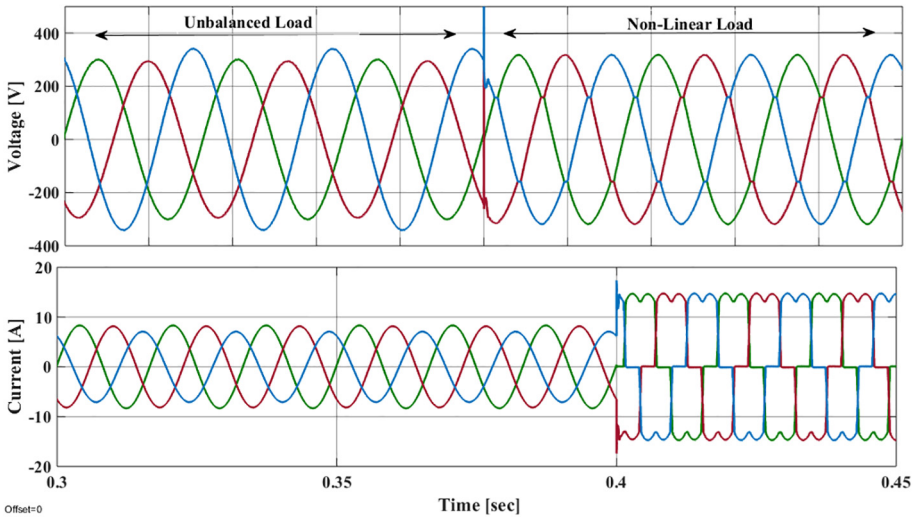

Fig. 12. Voltage and current results under non-linear and unbalanced loads using PI controller.

Table 5
THD comparison among the implemented control techniques.

	Linear load	Non-linear load
PI controller	3.53%	12.16%
Single-objective CF MPC	0.89%	1.40%
Dual-objective CF MPC	1.09%	–

formed. Fig. 10 shows that at time t = 0.12s, the non-linear load connected to the system becomes double. It can be noted that the output voltage waveform remains sinusoidal but shows a ditch during switching period as depicted in Fig. 10.

At t = 5 ms, the non-linear load is connected with system and at same time, the connected unbalanced load is disconnected to show the transition between different loading conditions. It is seen in Figs. 11(b) and 12(b) that the current becomes distorted because non-linear load is switched on. Fig. 12(a) demonstrates that the linear controller is unable to suppress the harmonics so, the quality of the output voltage becomes bad. But, the proposed control approach handles the non-linearity and the harmonics in output voltage is less, as presents in Fig. 12(a).

Table 5 present the comparison of the control strategy, discussed in this study in the form of total harmonic distortion (THD). THD is calculated using SIMULINK build-in FFT tool. Highest THD under both loading conditions is observed in the case of linear control. while single objective CF based MPC has lowest value of THD. In the case of dual objective CF, There is trade off between control parameter such as voltage and current. Slightly Increase the voltage THD but limit the current under fault conditions.

6.3. Multiple DGs: results and discussion

After validation of the proposed control for single DER. Now finally, this technique is tested for two DGs connected in parallel to serve a single load. Simulation is done in MATLAB/Simulink environment. Droop control strategy is employed for the better regulation of power between the DGs. The features of power-sharing and load transients are being investigated. Power sharing among the DERs is presented in Fig. 13. At 30 ms, the total system load doubles. Consequently, power generated by DGs also grows by the same rate to meet the system demand. Fig. 13(a), (b), (e) and (f) illustrate the load current and output voltage of DG_1 and DG_2. It is shown that at t = 0.03s, due to the increase in demand, the current of both inverters increases, while the voltage remains stable. Active and reactive power is equally shared by the droop control because both DGs have equal KVA rating as demonstrated in 13.

6.3.1. Dual objective CF under faults conditions

This section present the simulation results of PI controller, single objective CF based MPC and then for dual objective CF based MPC under symmetrical faults. In literature, many research studies have been found to address the faults but in mainly studies, sec-

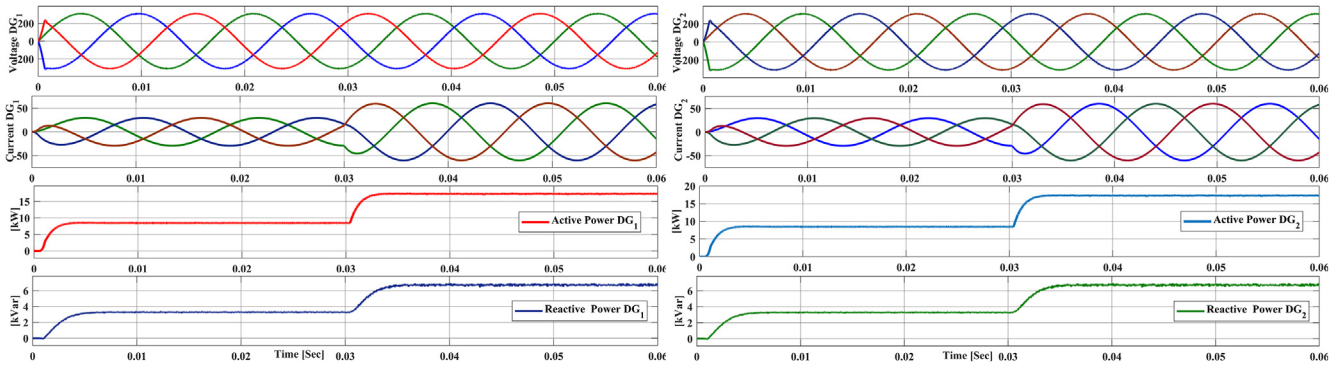

Fig. 13. Voltage, load current, active and reactive power of both DG_1 and DG_2 under load transients.

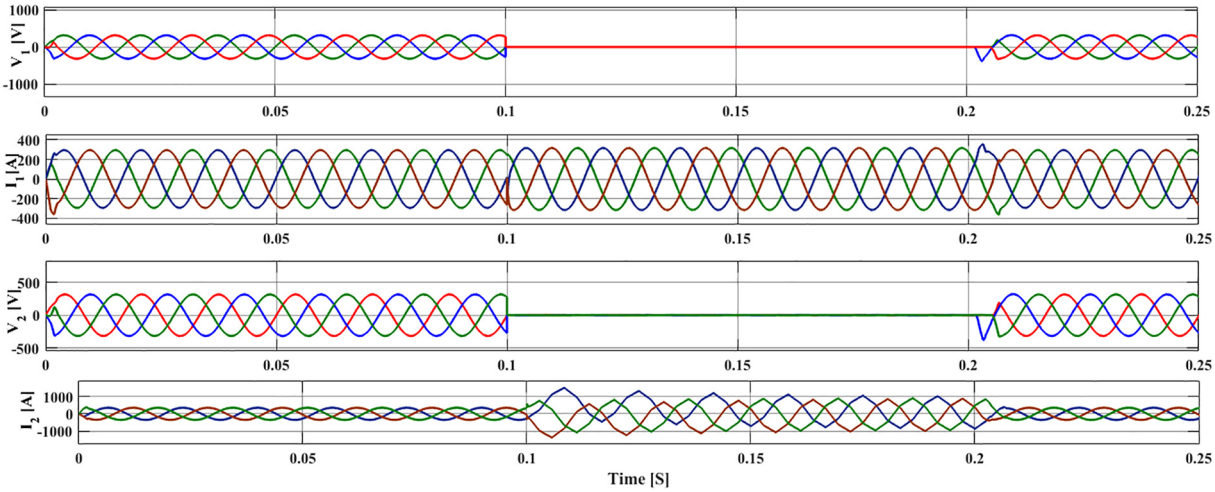

Fig. 14. Voltage and load current waveform of both DG_1 and DG_2 during 3-phase fault period.

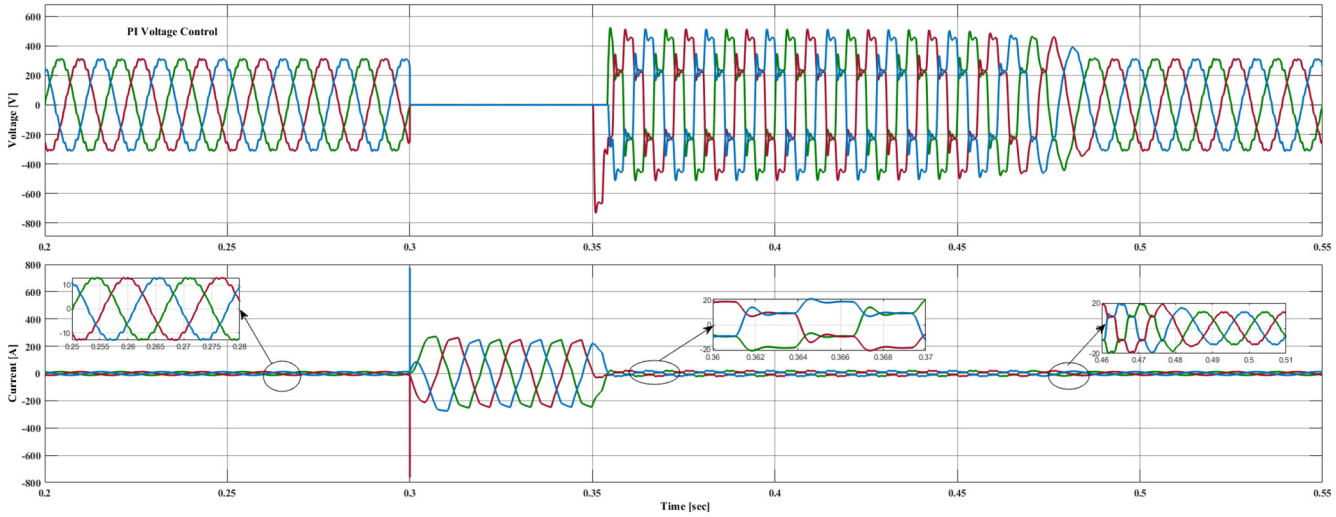

Fig. 15. Voltage and load current waveform of PI controller during 3-phase fault period.

ondary controller or hardware based devices is used to limit the fault current. However, authors don't find any literature to address this issue using converter basic control.In the dual objective CF,the primary objective of CF is to regulate the bus voltage and secondary function of CF is to compensate the output current under three-phase line to ground fault. However, the use of secondary term deteriorate the performance of controller in term of THD But advantages are far superior than the cons. In this scenario, a novel dual-objective CF is employed on DG_1. But the DG_2 having the single objective CF as described in (18).

14 illustrates the performance of newly designed dual-objective cost function in comparison with single objective CF. Output volt-

Table 6
Comparison of different control techniques.

References	Techniques Investigated	Voltage quality under Linear load (THD)	Voltage quality under Non-linear load (THD)	Controller implementation Complexity	Application
[16]	Proportional-Integral	9	30	Low	MG (Islanded), UPS
[17]	Proportional-Resonant	1.4	4.6	Low	MG,UPS
[19]	Dead-beat	2.1	4.8	Medium	MG, UPS
[26]	Slide Mode Control	Not given	2.66	High	General
[42]	Model Predictive Control	5.1	6.7	High	General
[30]	Observer-based MPC	2.82	3.8	Medium	UPS, MG (Islanded)
[33]	MPC (Implicit)	2.93	Not Given	Medium	General
[27]	ANN-MPC	1.09	2.89	High	General
Proposed	Improved FCS-MPC	**0.89**	**1.40**	Medium	MG (Islanded), UPS

age THD is more in the case of DG_1 as compared to DG_2 as shown in the Fig. 14. At t = 0.1s, three-phase line to ground fault occurs in the system, the voltage of the both DGs becomes zero and the load current of system rises and becomes distorted simultaneously, but at same time the current waveform of DG_1 remains sinusoidal and the current of the system increases but remains in safe limit. But the current of DG_2 increases by 3× of the load current.

15 illustrates the results of PI controller under fault condition. It is shown in the Fig.15 that at time 0.3s, a symmetrical phase is introduced in the system.The voltage og the system becomes zero but current shows a large spike. Fault is cleared at 0.35s, But the voltage and current of the system remains distorted and amplitude of the voltage is much higher than the reference. So, the controller is not following the reference and behave like as in transient period. PI controller takes 0.13s to becomes stables and works smoothly. All the simulation results verify that proposed MPC has better performance than any other classical controller.

Table 6 presents the comparison among the existing linear and non-linear control techniques found in literature with proposed control technique. The control approach under investigation demonstrates a better dynamic response and it effectively suppresses the harmonics and has excellent performance in comparison to the other controllers found in literature.

7. Conclusion

In this paper, a new dual objective CF-based FCS-MPC control technique has been studied for a single and multiple DGs in AC MG. The effectiveness of the proposed control technique has been verified by doing extensive simulations in the MATLAB/Simulink. Results based on simulations demonstrate that the proposed strategy attain excellent voltage regulation under linear and non-linear loads. Fault current is also regulated by a new CF under fault condition. The proposed controller does not need any external or internal parameters for adjustment. It only requires the system model in order to anticipate the state variables. Additionally, no modulator is required, thus the gate signals are directly provided by the controller. The proposed controller provides flexibility and eliminates the cascaded configuration to control the output voltage directly. Results are compared with conventional MPC and PI controllers. The proposed model demonstrates a significant decrease in the THD of the system and the switching frequency. Results also indicate that the output current remains sinusoidal under symmetrical faults. For proper power-sharing between the DGs in AC MG, Droop strategy is employed. The results depict perfect power regulation among the DERs in different loading conditions.

Declaration of Competing Interest

The authors declare that they have no known competing financial interests or personal relationships that could have appeared to influence the work reported in this paper.

Acknowledgment

The authors would like to thank the editors and anonymous reviewers for providing insightful suggestions and comments to improve the quality of research paper.

References

[1] W. Saad, Z. Han, H.V. Poor, T. Basar, Game-theoretic methods for the smart grid: an overview of microgrid systems, demand-side management, and smart grid communications, IEEE Signal Process. Mag. 29 (5) (2012) 86–105. URL: https://doi.org/10.1109/MSP.2012.2186410.

[2] A.G. Madureira, J.P. Lopes, Coordinated voltage support in distribution networks with distributed generation and microgrids, IET Renew. Power Gen. 3 (4) (2009) 439–454. URL:https://doi.org/10.1049/iet-rpg.2008.0064.

[3] M. Mumtaz, H.S. Khan, M. Aamir, M. Ali, A. Rehman, Load flow analysis of cigre benchmark model using etap, in: Proceedings of the International Conference on Renewable, Applied and New Energy Technologies, ICRANET, pp. 19–22..

[4] M. Aamir, K.A. Kalwar, S. Mekhilef, Uninterruptible power supply (ups) system, Renew. Sustain. Energy Rev. 58 (2016) 1395–1410. URL:https://doi.org/10.1016/j.rser.2015.12.335..

[5] H. Bakir, A.A. Kulaksiz, Modelling and voltage control of the solar-wind hybrid micro-grid with optimized statcom using ga and bfa, Eng. Sci. Technol. Int. J. 23 (3) (2020) 576–584. URL:https://doi.org/10.1016/j.jestch.2019.07.009.

[6] T. Dragicevic, X. Lu, J.C. Vasquez, J.M. Guerrero, Dc microgrids–part i: a review of control strategies and stabilization techniques, IEEE Trans. Power Electron. 31 (7) (2016) 4876–4891. URL:https://doi.org/10.1109/TPEL.2015.2478859.

[7] C. Chellaswamy, L. Balaji, T. Kaliraja, Renewable energy based automatic recharging mechanism for full electric vehicle, Eng. Sci. Technol. Int. J. 23 (3) (2020) 555–564. URL:https://doi.org/10.1016/j.jestch.2019.07.007.

[8] X. Liu, P. Wang, P.C. Loh, A hybrid ac/dc microgrid and its coordination control, IEEE Trans. Smart Grid 2 (2) (2011) 278–286. URL:https://doi.org/10.1109/TSG.2011.2116162.

[9] U. Datta, A. Kalam, J. Shi, Frequency performance analysis of multi-gain droop controlled dfig in an isolated microgrid using real-time digital simulator, Eng. Sci. Technol. Int. J. 23 (5) (2020) 1028–1041. URL:https://doi.org/10.1016/j.jestch.2019.11.008.

[10] X. Sun, Y.S. Lee, D. Xu, Modeling, analysis, and implementation of parallel multi-inverter systems with instantaneous average-current-sharing scheme, IEEE Trans. Power Electron. 18 (3) (2003) 844–856. URL:https://doi.org/10.1109/TPEL.2003.810867.

[11] Y.J. Cheng, E.K.K. Sng, A novel communication strategy for decentralized control of paralleled multi-inverter systems, IEEE Trans. Power Electron. 21 (1) (2006) 148–156. URL:https://doi.org/10.1109/TPEL.2005.861194.

[12] T. Caldognetto, P. Tenti, Microgrids operation based on master–slave cooperative control, IEEE J. Emerg. Select. Top. Power Electron. 2 (4) (2014) 1081–1088. URL:https://doi.org/10.1109/JESTPE.2014.2345052.

[13] J.M. Guerrero, L. Hang, J. Uceda, Control of distributed uninterruptible power supply systems, IEEE Trans. Industr. Electron. 55 (8) (2008) 2845–2859. URL: https://doi.org/10.1109/TIE.2008.924173.

[14] M.M.A. Abdelaziz, M.F. Shaaban, H.E. Farag, E.F. El-Saadany, A multistage centralized control scheme for islanded microgrids with pevs, IEEE Trans. Sustain. Energy 5 (3) (2014) 927–937. URL:https://doi.org/10.1109/TSTE.2014.2313765.

[15] U.B. Tayab, M.A.B. Roslan, L.J. Hwai, M. Kashif, A review of droop control techniques for microgrid, Renew. Sustain. Energy Rev. 76 (2017) 717–727. URL:https://doi.org/10.1016/j.rser.2017.03.028.

[16] P.C. Loh, M.J. Newman, D.N. Zmood, D.G. Holmes, A comparative analysis of multiloop voltage regulation strategies for single and three-phase ups systems, IEEE Trans. Power Electron. 18 (5) (2003) 1176–1185. URL: https://doi.org/10.1109/TPEL.2003.816199.

[17] A. Hasanzadeh, O.C. Onar, H. Mokhtari, A. Khaligh, A proportional-resonant controller-based wireless control strategy with a reduced number of sensors for parallel-operated upss, IEEE Trans. Power Delivery 25 (1) (2010) 468–478. URL:https://doi.org/10.1109/TPWRD.2009.2034911.

[18] S. Golestan, J.M. Guerrero, J.C. Vasquez, A pll-based controller for three-phase grid-connected power converters, IEEE Trans. Power Electron. 33 (2) (2018) 911–916. URL:https://doi.org/10.1109/TPEL.2017.2719285.

[19] P. Mattavelli, An improved deadbeat control for ups using disturbance observers, IEEE Trans. Industr. Electron. 52 (1) (2005) 206–212. URL: https://doi.org/10.1109/TIE.2004.837912.

[20] M.A.U. Rasool, M.M. Khan, M.T. Faiz, S. Tahir, W. Zhang, An optimized disturbance observer based digital deadbeat control technique for three-phase voltage source inverter (2018). doi: 10.1145/3277453.3286094. URL: https://doi.org/10.1145/3277453.3286094.

[21] M. Ali, M. Aamir, H.S. Khan, A. Waqar, F. Haroon, A.R. Jafri, Lyapunov stability and performance analysis of the fractional order sliding mode control for a parallel connected ups system under unbalanced and nonlinear load conditions, Energies 11 (12) (2018) 3475. URL:https://doi.org/10.3390/en11123475.

[22] O. Kukrer, H. Komurcugil, A. Doganalp, A three-level hysteresis function approach to the sliding-mode control of single-phase ups inverters, IEEE Trans. Industr. Electron. 56 (9) (2009) 3477–3486. URL:https://doi.org/10.1109/TIE.2009.2016512.

[23] M.A.U. Rasool, M.M. Khan, Z. Ahmed, M.A. Saeed, Analysis of an h8 robust control for a three-phase voltage source inverter, Inventions 4 (1) (2019) 18. URL:https://doi.org/10.3390/inventions4010018.

[24] C.K. Sao, P.W. Lehn, Autonomous load sharing of voltage source converters, IEEE Trans. Power Delivery 20 (2) (2005) 1009–1016. URL:https://doi.org/10.1109/TPWRD.2004.838638.

[25] M. Ali, M. Aamir, H.S. Khan, A.A. Khan, F. Haroon, Design and implementation of fractional-order sliding mode control for parallel distributed generations units in islanded microgrid, in: 2019 IEEE 28th International Symposium on Industrial Electronics (ISIE), IEEE, pp. 64–69. URL:https://doi.org/10.1109/ISIE.2019.8781383..

[26] H. Komurcugil, Rotating-sliding-line-based sliding-mode control for single-phase ups inverters, IEEE Trans. Industr. Electron. 59 (10) (2012) 3719–3726. URL:https://doi.org/10.1109/TIE.2011.2159354..

[27] I.S. Mohamed, S. Rovetta, T.D. Do, T. Dragicevic, A.A.Z. Diab, A neural-network-based model predictive control of three-phase inverter with an output *lc*, IEEE Access 7 (2019) 124737–124749. URL:https://doi.org/10.1109/ACCESS.2019.2938220.
[28] W. Lu, K. Zhou, D. Wang, M. Cheng, A general parallel structure repetitive control scheme for multiphase dc–ac pwm converters, IEEE Trans. Power Electron. 28 (8) (2013) 3980–3987. URL:https://doi.org/10.1109/TPEL.2012.2229395.
[29] H.K. Kang, C.H. Yoo, I.Y. Chung, D.J. Won, S.I. Moon, Intelligent coordination method of multiple distributed resources for harmonic current compensation in a microgrid, J. Electr. Eng. Technol. 7 (6) (2012) 834–844. URL:https://doi.org/10.5370/JEET.2012.7.6.834.
[30] P. Cortés, G. Ortiz, J.I. Yuz, J. Rodríguez, S. Vazquez, L.G. Franquelo, Model predictive control of an inverter with output *lc* filter for ups applications, IEEE Trans. Industr. Electron. 56 (6) (2009) 1875–1883. URL:https://doi.org/10.1109/TIE.2009.2015750.
[31] C. Zheng, T. Dragicevic, F. Blaabjerg, Current-sensorless finite-set model predictive control for lc-filtered voltage source inverters, IEEE Trans. Power Electron. URL:https://doi.org/10.1109/TPEL.2019.2914452..
[32] K.H. Ahmed, A.M. Massoud, S.J. Finney, B.W. Williams, A modified stationary reference frame-based predictive current control with zero steady-state error for lcl coupled inverter-based distributed generation systems, IEEE Trans. Industr. Electron. 58 (4) (2011) 1359–1370. URL:https://doi.org/10.1109/TIE.2010.2050414.
[33] M. Nauman, A. Hasan, Efficient implicit model-predictive control of a three-phase inverter with an output lc filter, IEEE Trans. Power Electron. 31 (9) (2016) 6075–6078. URL:https://doi.org/10.1109/TPEL.2016.2535263.
[34] H.S. Khan, M. Aamir, M. Ali, A. Waqar, S.U. Ali, J. Imtiaz, Finite control set model predictive control for parallel connected online ups system under unbalanced and nonlinear loads, Energies 12 (4) (2019) 581, https://doi.org/10.3390/en12040581.
[35] C. Zheng, T. Dragicevic, B. Majmunovic, F. Blaabjerg, Constrained modulated-model predictive control of an lc)filtered voltage source converter, IEEE Trans. Power Electron. URL:https://doi.org/10.1109/TPEL.2019.2917634..
[36] C.A. Plet, T.C. Green, A method of voltage limiting and distortion avoidance for islanded inverter-fed networks under fault, in: Proceedings of the 2011 14th European Conference on Power Electronics and Applications, IEEE, pp. 1–8..
[37] E. Ebrahimi, G. Gharehpetian, J. Milimonfared, A novel scheme to protect distribution networks in presence of inverter-based distributed generation, in: International Conference on Renewable Energies and Power Quality..
[38] I. Sadeghkhani, M.E.H. Golshan, J.M. Guerrero, A. Mehrizi-Sani, A current limiting strategy to improve fault ride-through of inverter interfaced autonomous microgrids, IEEE Trans. Smart Grid 8 (5) (2016) 2138–2148.
[39] X. Pei, Y. Kang, Short-circuit fault protection strategy for high-power three-phase three-wire inverter, IEEE Trans. Industr. Inf. 8 (3) (2012) 545–553.
[40] I. Ngamroo, T. Karaipoom, Improving low-voltage ride-through performance and alleviating power fluctuation of dfig wind turbine in dc microgrid by optimal smes with fault current limiting function, IEEE Trans. Appl. Superconduct. 24 (5) (2014) 1–5.
[41] J. Hu, J. Zhu, D.G. Dorrell, Model predictive control of grid-connected inverters for pv systems with flexible power regulation and switching frequency reduction, IEEE Trans. Ind. Appl. 51 (1) (2015) 587–594. URL:https://doi.org/10.1109/TIA.2014.2328785.
[42] V. Yaramasu, M. Rivera, M. Narimani, B. Wu, J. Rodriguez, Rodriguez, Model predictive approach for a simple and effective load voltage control of four-leg inverter with an output *lc* filter, IEEE Trans. Industr. Electron. 61 (10) (2014) 5259–5270. URL:https://doi.org/10.1109/TIE.2013.2297291.

Hussain Sarwar Khan is born in Muzaffargarh, Pakistan in 1994. He received the B. Sc. degrees in electrical (Power) engineering from the Islamia University of Bahawalpur, Pakistan in 2016 and completed the master studies degree in electrical engineering with specialization in power systems from Bahria University Islamabad, Pakistan in 2018.

From 2017 to 2018, he was a Design Engineer (R&D) at a research project funded by Higher Education Commission, Pakistan at Bahria University Islamabad. He is currently serving as a Project Researcher at School of Technology and Innovations, University of Vaasa, Vaasa, Finland. His research interests include model predictive control, UPSs, control of power converter, renewable energy and microgrid.

Muhammad Aamir received the B.E. (Hons.) degree in electrical engineering from the University of Engineering and Technology (UET), Peshawar, Pakistan, in 2007, the Master's degree in electrical engineering from Hanyang University, Seoul, South Korea, in 2011 and Ph.D. degree in electrical engineering from Power Electronics and Renewable Energy Research Laboratory (PEARL), University of Malaya, Kuala Lumpur, Malaysia in 2016. He is currently working as Assistant Professor at Pak-Austria Fachhochschule Institute of Applied Sciences and Technology Haripur, Pakistan. His research interests include UPSs, power conversion, Microgrid and control of power converters.

Kimmo Kauhaniemi was born in Kankaanpaa, Finland, in 1963. He received the M. Sc. and Dr. Tech. degrees in electrical engineering from the Tampere University of Technology, Finland, in 1987 and1993, respectively. He was with the VTT Technical Research Centre of Finland. He is currently a Professor and the Head of the Smart Electric Systems (SES) Research Group in electrical engineering with the University of Vaasa, Finland. He has long-term experience on transient simulation of various power systems. His research interests include electricity distribution systems, relay protection, smart grids, and microgrids.

Muhammad Waqar Hassan was born in D. G. Khan, Pakistan in 1996. He received the B.Sc. and MS degrees in electrical (Power) engineering from the Islamia University of Bahawalpur, Pakistan in 2017 and 2020 respectively. Muhammad Waqar Hassan became a Member of Pakistan Engineering Council in 2017. His research interests are grid-tied inverter, power regulation, microgrid, and model predictive control.